Dynamical Simulation of Spins on Kagomé and Square Lattices

Amit Keren
Department of Physics, Columbia University, New York, New York 10027
(Received 7 January 1994)

The time evolution of classical Heisenberg spins on kagomé and square lattices is numerically evaluated. A clear difference is found between the two cases in the time dependence of an individual spin $S(t)$. The stability of possible ground states is discussed in light of the sample-averaged correlation function $[S(t)S(0)]$. The spectral density $j(\omega)$ as a function of temperature is also computed. In the square lattice two phases are observed, whereas in the kagomé lattice only motional narrowing is seen. The application of these simulations to $SrCr_8Ga_4O_{19}$ is discussed.

PACS numbers: 75.10.Jm, 75.40.Mg

The Heisenberg model with antiferromagnetic interaction between near neighbors on the kagomé lattice (Fig. 1) has drawn considerable attention due to the degeneracy of its ground states [1–8]. The energy of this system can be minimized by placing the spins on each triangle 120 degrees away from each other, which results in a manifold of possible ground states [2]. In some of these states the spins lie in one plane. At least two of these coplanar states also possess long range Néel order: the so-called $\sqrt{3}\times\sqrt{3}$ and $q=0$ states. The states with long range order are obtained by defining three spin orientations, A, B, and C, such that the angle between any two of them is 120 degrees. The $q=0$ configuration, shown in Fig. 1(a), is obtained by placing the spins along any line which connects nearest neighbors in an alternating sequence (e.g., $ABABAB$) [3]. The $\sqrt{3}\times\sqrt{3}$ state, shown in Fig. 1(b), is obtained by placing the spins along each such line in a rotating sequence (e.g., $ABCABCA$) [4]. However, minimizing the classical energy in itself does not necessarily cause the system to favor long range order or even a coplanar configuration. The selection of specific configurations must therefore proceed via some other mechanism.

Chalker *et al.* [5] argued that thermal fluctuations will cause the system to select a coplanar ground state (so-called order by disorder). They attribute this selection to zero mode excitations (a local motion of a small group of spins), found by Harris *et al.* [3]. Numerical simulations performed by Reimers and Berlinsky demonstrated that the tendency towards coplanarity starts at $T/J\sim 0.01$ [6]. The simulations also showed an increase in the order parameter corresponding to the $\sqrt{3}\times\sqrt{3}$ state ($m_{\sqrt{3}}$), as $T\to 0$. In addition, according to Sachdev, the $\sqrt{3}\times\sqrt{3}$ configuration is selected by quantum fluctuations [7]. However, some forces are detrimental to the $\sqrt{3}\times\sqrt{3}$ state. One such force is the decrease in free energy resulting from low concentration chiral domain walls [6]. Another force, discussed by von Delft and Henley, stems from tunneling phenomena which compete with the tendency towards long range order in the case of small integer spin [8]. The competition between mechanisms that favor the $\sqrt{3}\times\sqrt{3}$ state and those that drive the system towards disorder could result in interesting dynamical behavior.

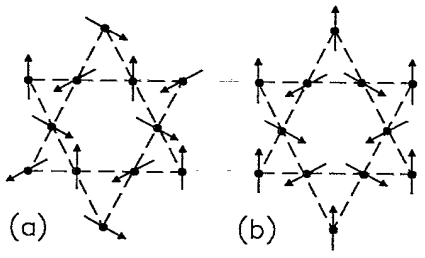

FIG. 1. Classical spins on the kagomé lattice with (a) a $q=0$ ground state and (b) a $\sqrt{3}\times\sqrt{3}$ ground state.

Experimentally, $SrCr_8Ga_4O_{19}$ (SCGO) has been studied as a physical realization of the kagomé system [9]. Neutron scattering and muon spin relaxation experiments have revealed very interesting dynamical behavior. In neutron scattering, at $T=1.5$ K, the frozen part of the moment was found to be less than half of the fluctuating part; the broad scattering peak was associated with short range antiferromagnetic correlation [10]. Spin fluctuations at 40 mK, without any detectable static component, were found in muon spin relaxation measurements [11]. Both of these measurements are sensitive to temporal spin fluctuations.

These dynamical properties, unusual from both a theoretical and experimental standpoint, motivated us to simulate the time evolution of spins on a kagomé lattice. Our aim is to check the stability of the long range order against excitation as well as to investigate the temperature dependence of the spin-spin correlation function. We also wish to examine the influence of the underlying lattice geometry on the spin evolution. We achieve this by comparing the dynamics of kagomé and square lattices, since both these lattices are fourfold coordinated. Our dynamical study proceeds in three steps: (I) we examine the time evolution of an individual spin $S_i(t)$ for given initial conditions, (II) we test the stability of the system by comparing the sample averaged correlation function $[S(0)S(t)]$ between the two lattices for a given excitation energy, and (III) we evaluate the spectral density

0031-9007/94/72(20)/3254(4)$06.00

$j(\omega)$ from the temperature averaged correlation function $\langle S(0)S(t)\rangle$ and discuss its application to experiments.

We approximate the equation of motion for each spin by that derived from the classical Heisenberg Hamiltonian, namely,

$$\frac{d\widehat{S}_i}{dt} = -J\widehat{S}_i \times \sum_{j:i} \widehat{S}_j, \qquad (1)$$

where $\widehat{S}_i$ is a three-component unit vector representing the spin direction. The sum in Eq. (1) is taken over the nearest neighbors of the ith spin (employing periodic boundary conditions). We numerically evaluate $\widehat{S}_i(t)$ for both a two dimensional (2D) kagomé lattice and a 2D square lattice using the fourth order Runge-Kutta (RK) algorithm with a time increment (dt) of 0.02 or less [12]. The lattice sizes in steps I and II are as follows: 972 spins ($L = 18$) for the kagomé, and 900 spins ($L = 30$) for the square. In step III we present results for the kagomé lattice with smaller sizes as well.

In step I the simulation is performed for a particular choice of excitation in (a) the square lattice, (b) the $\sqrt{3} \times \sqrt{3}$ state on the kagomé lattice, and (c) the $q = 0$ state on the kagomé lattice. We first place the spins in a long range ordered ground state where the spins lie in the $\widehat{x}\widehat{y}$ plane. We then pivot one spin out of this plane [$S_z(0) = 1$]. The excitation energy corresponding to this configuration is $4J$ on the square lattice and $2J$ on the kagomé lattice. The results are shown in Fig. 2. In each of the three cases, (a), (b), and (c), we present the time evolution of S_z for two different spins on the lattice: $\widehat{S}_z(t)$ of the modified spin and $\widehat{S}_z(t)$ of an unmodified spin. The figures demonstrate a remarkable difference between the time evolution of the spins on the square lattice and the spins on the kagomé lattice. In the square case, the modified spin undergoes periodic motion around an average value which lies in the plane. The frequency ($8\pi J$) of this motion corresponds to the field at the site of the modified spin at $t = 0$. The motion of the modified spin is governed by a narrow distribution of frequencies and is only weakly damped within the plotted simulation time. In the kagomé case, on the other hand, none of the spins can be described as fluctuating around a finite average component at long times. There is also more than one characteristic time scale involved in the motion. Only at the beginning of the motion can a frequency ($4\pi J$) be defined for three periods. This frequency again corresponds to the local field at the site of the modified spin at $t = 0$.

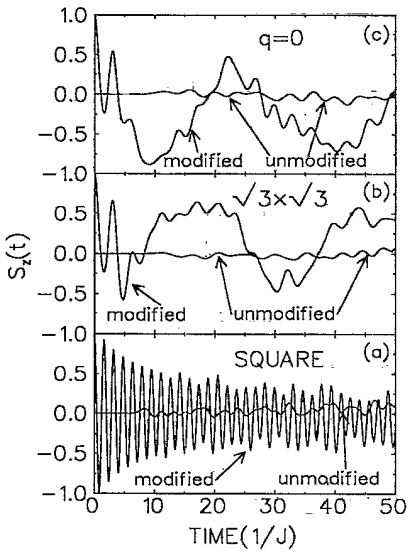

FIG. 2. The time evolution of $\widehat{S}_z$ in three cases: (a) The excited square lattice; (b) the excited $\sqrt{3} \times \sqrt{3}$ state on the kagomé lattice; (c) the excited $q = 0$ state on the kagomé lattice. The excitation of the system is achieved by rotating one spin into a direction perpendicular to the plane of the ground state. In each case $\widehat{S}_z(t)$ for both the modified spin and another, initially unmodified spin, is shown.

In step II we obtain the sample-averaged correlation function (SACF) for a given excitation energy. The SACF is calculated by evaluating the scalar product of $\widehat{S}_i(0)$ and $\widehat{S}_i(t)$ for each individual spin and then averaging over the entire lattice. Here, unlike in step I, we excite the system by slightly disorienting each spin on the lattice from its ground state orientation. The new orientation is chosen randomly within a small solid angle (Ω) centered around the original spin direction. The energy of excitation (ΔE) is controlled by the choice of Ω. In Fig. 3 we show the SACF with this type of collective excitation ($\Delta E = 4J$). The difference between the square and the kagomé lattice is obvious, but there is also a substantial difference between the $\sqrt{3} \times \sqrt{3}$ and the $q = 0$. We discuss the three cases in the frame-

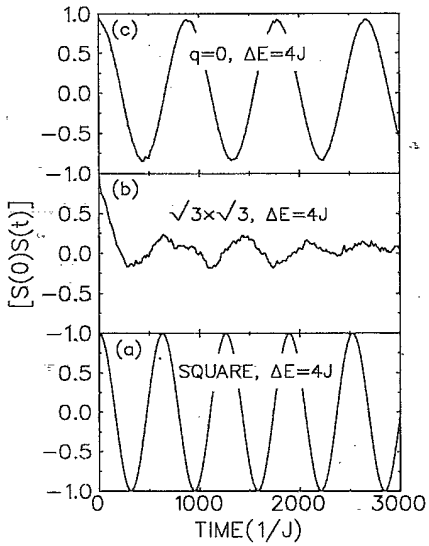

FIG. 3. Sample averaged correlation function for the collectively excited (a) square lattice, (b) $\sqrt{3} \times \sqrt{3}$ state on kagomé lattice, and (c) $q = 0$ state on kagomé lattice.

work of a damped harmonic oscillator. The SACF of the square lattice, shown in Fig. 3(a), exhibits a clearly defined frequency ($0.01J$) with a zero damping rate. On the other hand, the SACF in the excited $\sqrt{3} \times \sqrt{3}$ has a very large damping rate and oscillations occur on various time scales. Finally, the excited $q = 0$ is an intermediate case in which the frequency, like that of the square, is well defined ($0.007J$), but the damping is finite like that of the $\sqrt{3} \times \sqrt{3}$.

In step III we perform the temperature average following the procedure of Wysin and Bishop using a combination of Monte Carlo (MC) simulation and the RK integration [13]. The underlying equation which we evaluate is

$$\langle S(0)S(t)\rangle = \sum_{\mathrm{IC}} \frac{e^{(-E/T)}}{Z} [S(0)S(t)]_{\mathrm{IC}}\,, \qquad (2)$$

where IC stands for initial conditions, E is the total energy of the system, T is the temperature, and Z is the partition function. The evaluation of Eq. (2) is done in a cyclic procedure: first the system is warmed from the $T = 0$ configuration by MC; next, the final configuration of the MC procedure is taken to be the initial configuration for the equations of motion; the RK integration is then used to obtain a correlation function, and the final configuration of the motion is fed back into the MC for a new choice of initial conditions. We average the correlation functions over 18 cycles at low temperatures and 6 cycles at high temperatures. For the Monte Carlo selection of states we use 10 000 lattice sweeps in the standard Metropolis algorithm [12]. In the kagomé case, the $T = 0$ state is taken as the $\sqrt{3} \times \sqrt{3}$.

At the end of the temperature averaging we obtain the spectral density defined as

$$j(\omega) = 2\int_0^\infty dt \cos(\omega t)\, \langle S(0)S(t)\rangle\,, \qquad (3)$$

using a fast Fourier transform (FFT) algorithm. The weak damping rate in the oscillations of the square case hinders the Fourier transform and we have to smooth the spectra with a Gaussian. The details of the shape of $j(\omega)$ therefore depend on the choice of Gaussian and the simulation time. However, the quantity which is of major concern to us, $j(0)$, only weakly depends on the transformation procedure. In the kagomé case, there is no difficulty in obtaining the Fourier transform.

In Figs. 4(a)–4(c) we show $j(\omega)$ for the square lattice at three temperatures: 1, 0.1, and $0.02J$. The reader should note the different time scales of the abscissa. As the temperature decreases from 1.0 to 0.1, the scale of the spectral density narrows and $j(0)$ increases. In addition, a number of spin wavelike peaks appear in the spectra. The narrowing of the spectral density with decreasing temperature is characteristic of a paramagnetic phase. Upon further cooling to $0.02J$, $j(0)$ decreases and only one narrow peak centered at $\omega > 0$ is observed. This behavior is characteristic of an ordered phase and

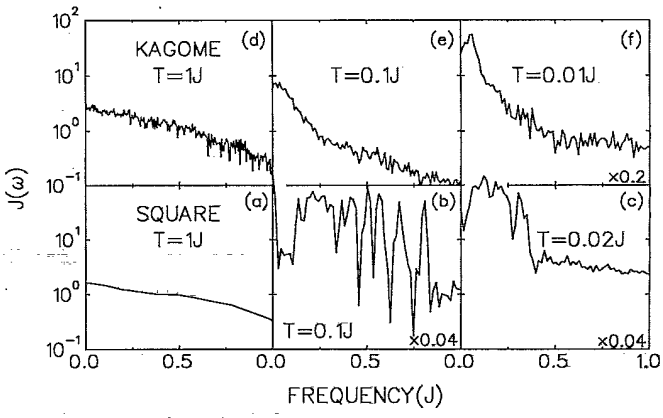

FIG. 4. Spectral density $j(\omega)$ in the square lattice obtained at (a) $T = 1.0J$, (b) $T = 0.1J$, and (c) $T = 0.02J$, and in the kagomé lattice obtained at (d) $T = 1.0J$, (e) $T = 0.1J$, and (f) $T = 0.01J$.

can be qualitatively understood from the results of step II. At low temperatures, only a narrow range of low energy excitations are accessible to the system; the correlation function is therefore combined from a number of $[S(0)S(t)]$ which resemble each other. The SACF shown in Fig. 3(a) is a typical example of one such $[S(0)S(t)]$. It results in a $\langle S(0)S(t)\rangle$ which can be described as an underdamped oscillator and a spectral density with a peak at $\omega > 0$. At high temperatures a wide range of high energy excitations are accessible to the system; the correlation function is expected to be overdamped and the maximum of $j(\omega)$ is expected at $\omega = 0$. In the kagomé lattice the situation is fundamentally different, as can be seen from Figs. 4(d)–4(f). Although there is a narrowing of the spectral density, $j(0)$ continuously increases upon cooling. In other words, no phase transition is seen as $T \to 0$. This behavior can also be understood from step II; the SACF in the $\sqrt{3} \times \sqrt{3}$ shown in Fig. 3(b) is strongly damped even at very low excitation energies. It is therefore not surprising that $\langle S(0)S(t)\rangle$ is overdamped and that $j(\omega)$ is peaked at zero frequency for all temperatures.

In Fig. 5 we show $j(0)$ [normalized by the value of $j(0)$ at $T = 10J$] as a function of temperature for the kagomé and square lattices. The error bars are estimated from the variation of $j(0)$ between different cycles. In this figure we also show simulation results for a kagomé lattice with 675 ($L = 15$) spins and 108 ($L = 6$) spins. In the square lattice we see a maximum in $j(0)$ at $T = 0.1J$, while in the kagomé lattice, $j(0)$ is monotonically increasing with decreasing temperature. In addition, we see a very weak lattice-size dependence in the kagomé case. The peak of $j(0)$ in the square case is not surprising, since at $T \sim 0.5J$ the correlation length reaches the lattice size [14]. However, the continuous increase of $j(0)$ in the kagomé case, even for a small system, is not trivial, especially in view of the increase in the order parameter

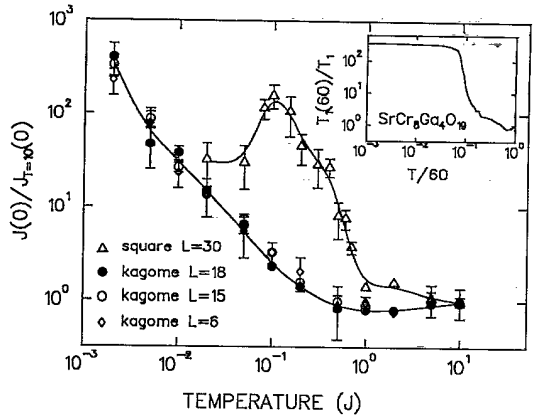

FIG. 5. The spectral density at zero frequency $j(0)$ normalized by the value of $j(0)$ at $T = 10.0J$ is plotted against temperature in units of J. The normalization factors are $1.12/J$ in the square with $L = 30$ spins, $2.40/J$ in the kagomé with $L = 18$ spins, $2.36/J$ in the kagomé with $L = 15$ spins, and $1.17/J$ in the kagomé with $L = 6$ spins. The solid lines are guides for the eye. The inset shows the experimental result for the μ^+ spin-lattice relaxation as a function of temperature in $SrCr_8Ga_4O_{19}$ [11].

$m_{\sqrt{3}}$ with decreasing lattice size at $T \to 0$ [6]. It suggests that the difference between the square and kagomé lattices is due to the local motion of spins in the kagomé system, namely, the zero modes.

The spectral density at zero frequency, $j(0)$, is intimately related to the spin-lattice relaxation rate (T_1) of local probes (e.g., NMR and μSR). The relation, when the static local field is small, is given by $1/T_1 \sim B^2 j(0)$ where B is the instantaneous local field at the probe site [15]. From our simulation we therefore anticipate the absence of a T_1 minimum in the kagomé lattice. Indeed, such an absence was observed in the kagomé system $SrCr_8Ga_4O_{19}$ using the μSR technique [11]. The experimental results, normalized by $J = 60$ K [3], are presented in the inset of Fig. 5. It should be noted that some differences between these simulations and the μSR experiment on SCGO are anticipated since SCGO contains 14% nonmagnetic impurities on the kagomé plane as well as magnetically active triangular planes.

We have found that the kagomé lattice has a very strong influence on the evolution of Heisenberg spins. Between the two kagomé ground states discussed here, the $q = 0$ is more stable against small excitations. In the $\sqrt{3} \times \sqrt{3}$ state the system loses memory of its initial configuration relatively quickly. Our simulations demonstrate that in the kagomé lattice the spectral density continuously narrows with no transition down to $T = 0$. This is in agreement with both experimental results and thermodynamical simulations [5]. We also demonstrate that the kagomé lattice and possibly other frustrated magnets are good candidates for the type of dynamical studies presented here.

The author wishes to thank A. S. Blaer, V. Elser, M. Gingras, K. Kojima, G. M. Luke, S. Miyashita, O. Tchernyshyov, W. D. Wu, and Y. J. Uemura for helpful discussions.

[1] D. A. Huse and A. D. Rutenberg, Phys. Rev. B **45**, 7536 (1992); R. R. P. Singh and D. A. Huse, Phys. Rev. Lett. **68**, 1766 (1992); A. Chubukov, Phys. Rev. Lett. **69**, 832 (1992); P. W. Leung and V. Elser, Phys. Rev. B **47**, 5459 (1993); V. Elser and C. Zeng, Phys. Rev. B **48**, 13647 (1993), and references therein.

[2] E. F. Shender, V. B. Cherepanov, P. C. W. Holdsworth, and A. J. Berlinsky, Phys. Rev. Lett. **70**, 3812 (1993).

[3] A. B. Harris, C. Kallin, and J. Berlinsky, Phys. Rev. B **45**, 2899 (1992).

[4] C. Zeng and V. Elser, Phys. Rev. B **42**, 8436 (1990).

[5] J. T. Chalker, P. C. W. Holdsworth, and E. F. Shender, Phys. Rev. Lett. **68**, 855 (1992).

[6] Jan N. Reimers and A. J. Berlinsky, Phys. Rev. B **48**, 9539 (1993).

[7] S. Sachdev, Phys. Rev. B **45**, 12377 (1992).

[8] J. von Delf and C. L. Henley, Phys. Rev. B **48**, 965 (1993).

[9] A. P. Ramirez, G. P. Espinosa, and A. S. Cooper, Phys. Rev. Lett. **64**, 2070 (1990); A. P. Ramirez, G. P. Espinosa, and A. S. Cooper, Phys. Rev. B **45**, 2505 (1992); B. Martínez *et al.*, Phys. Rev. B **46**, 10786 (1992).

[10] C. Broholm, G. Aeppli, G. P. Espinosa, and A. S. Cooper, Phys. Rev. Lett. **65**, 3173 (1990); G. Aeppli, C. Broholm, A. Ramirez, G. P. Espinosa, and A. S. Cooper, J. Magn. Magn. Mater. **90&91**, 225 (1990).

[11] A. Keren *et al.*, in Proceedings of the μSR'93 Conference, June 1993, Maui [Hyperfine Interact. (to be published)]; Y. J. Uemura, A. Keren, L. P. Le, G. M. Luke, B. J. Sternlieb, and W. D. Wu, *ibid.*

[12] W. H. Press, B. P. Flannery, A. A. Teukolsky, and W. T. Vetterling, *Numerical Recipes* (Cambridge University Press, Cambridge, 1989).

[13] G. M. Wysin and A. R. Bishop, Phys. Rev. B **42**, 810 (1990).

[14] H. Shenker and J. Tobochnik, Phys. Rev. B **22**, 4462 (1980).

[15] T. Moriya, Progr. Theor. Phys. **28**, 371 (1962).